SE

PORT DOCUMENTATION PAGE DTIC FILE COPY

1a. AD-A224 693	1b RESTRICTIVE MARKINGS

2a. SECURITY CLASSIFICATION AUTHORITY	3. DISTRIBUTION/AVAILABILITY OF REPORT
2b. DECLASSIFICATION/DOWNGRADING SCHEDULE	Approved for public release; distribution unlimited

4. PERFORMING ORGANIZATION REPORT NUMBER(S)	5. MONITORING ORGANIZATION REPORT NUMBER(S)
Technical Report #16	

6a. NAME OF PERFORMING ORGANIZATION	6b. OFFICE SYMBOL (If applicable)	7a. NAME OF MONITORING ORGANIZATION
SUNY/Buffalo		Office of Naval Research

6c. ADDRESS (City, State, and ZIP Code)	7b. ADDRESS (City, State, and ZIP Code)
Dept. of Chemistry, Acheson Hall, SUNY/Buffalo, Buffalo, NY 14214	Chemistry Program 800 N. Quincy St., Arlington, VA 22217

8a. NAME OF FUNDING/SPONSORING ORGANIZATION	8b. OFFICE SYMBOL (If applicable)	9. PROCUREMENT INSTRUMENT IDENTIFICATION NUMBER
Office of Naval Research		#N00014-88-K-0483

8c. ADDRESS (City, State, and ZIP Code)	10. SOURCE OF FUNDING NUMBERS			
Chemistry Program, 800 N. Quincy St., Arlington, VA 22217	PROGRAM ELEMENT NO.	PROJECT NO.	TASK NO.	WORK UNIT ACCESSION NO

11. TITLE (Include Security Classification)

CHEMISTRY WITHIN MOLECULAR VAN DER WAALS CLUSTERS

12. PERSONAL AUTHOR(S)
James F. Garvey, William R. Peifer and M. Todd Coolbaugh

13a. TYPE OF REPORT	13b. TIME COVERED	14. DATE OF REPORT (Year, Month, Day)	15. PAGE COUNT
Technical	FROM _____ TO _____		29

16. SUPPLEMENTARY NOTATION

Accounts of Chemical Research

17.	COSATI CODES		18. SUBJECT TERMS (Continue on reverse if necessary and identify by block number)
FIELD	GROUP	SUB-GROUP	

19. ABSTRACT (Continue on reverse if necessary and identify by block number)

An invited review article which document the progress we have made for the past three yearsat the University of Buffalo (under ONR support!)

DTIC
S ELECTE D
AUG 0 2 1990
D

20. DISTRIBUTION/AVAILABILITY OF ABSTRACT	21. ABSTRACT SECURITY CLASSIFICATION
☒ UNCLASSIFIED/UNLIMITED ☐ SAME AS RPT. ☐ DTIC USERS	Unclassified

22a. NAME OF RESPONSIBLE INDIVIDUAL	22b. TELEPHONE (Include Area Code)	22c. OFFICE SYMBOL
Dr. David L. Nelson	(202) 696-4410	

DD FORM 1473, 84 MAR   83 APR edition may be used until exhausted.   SECURITY CLASSIFICATION OF THIS PAGE
All other editions are obsolete.

90 08 01 001

OFFICE OF NAVAL RESEARCH

GRANT N00014-88-K-0493

R & T Code 412m008

Technical Report No. 16

CHEMISTRY WITHIN
MOLECULAR VAN DER WAALS CLUSTERS

by

James F. Garvey*, William R. Peifer and M. Todd Coolbaugh

Invited Publication
in
Accounts of Chemical Research

Acheson Hall
Department of Chemistry
University at Buffalo
The State University of New York at Buffalo
Buffalo, NY
14214

Chemistry within
Molecular van der Waals Clusters

James F. Garvey*, William R. Peifer, and M. Todd Coolbaugh

Acheson Hall, Department of Chemistry

State University of New York at Buffalo

Buffalo, NY 14214

James F. Garvey was born in Passaic, NJ, in 1957. After receiving his B.S./M.S. from Georgetown University he then went on to get his Ph.D from the California Institute of Technology in 1985 under Aron Kuppermann. He spent the following two years as a post-doctoral fellow at UCLA, with Richard Bernstein, and it was there he became interested in looking at ion-molecule reactions within clusters. In 1987 he joined the faculty at SUNY/Buffalo where he is continuing to pursue research in this area.

William R. Peifer received his B.S. from U. C. Davis in 1979 and, after a few years of employment in the public and private sectors, returned to UCD to receive his Ph.D with Robert N. Rosenfeld in 1986. He did postdoctoral work with Albert C. Parr at NBS before moving to Buffalo for postdoctoral work with James F. Garvey.

M. Todd Coolbaugh was born in Elmira, NY in 1962. He received his B.A. from Alfred University in 1985 and is currently completing his Ph.D work at SUNY/Buffalo.

A) Introduction

B) Experimental Section

C) Results and Discussion

    1) Stabilizing an Unstable Reagent within a Cluster

        a) 1,1-Difluoroethane Clusters

    2) Providing New Chemical Pathways

        a) Ammonia Clusters

        b) Ethylene Clusters

        c) Ar-Methanol Clusters

        d) Metal Hexacarbonyl Clusters

    3) Stabilizing an Unstable Intermediate within a Cluster

        a) Dimethyl Ether Clusters

        b) Photodissociation of $Cr(CO)_6$ within Methanol Clusters

D) Future Directions

A) Introduction

A subject of great interest in recent years has been the study of the physics of weakly bound van der Waals clusters. These species have been probed in a variety of ways to gain an understanding of their formation and to determine their various physical properties. However, the study of chemical reactions within clusters is especially intriguing since clusters can conceptually bridge the disparate fields of bimolecular gas-phase reaction dynamics and solution chemistry. The ultimate goal of these studies is to obtain an understanding of the factors that govern reactions in solution but which are absent in gas phase processes. By concentrating on the chemistry within these cluster systems it is possible to directly observe how the behavior of the system changes as a function of stepwise solvation.

Most of the recent work in this area consists of utilizing a neutral cluster as one of the reagents for a bimolecular reaction[1-8] with the product cluster ion being directly detected via conventional mass spectrometric techniques. Apart from the observation of protonated clusters {i.e., $(H_2O)_nH^+$,[9] $(NH_3)_nH^+$,[10,11] $(CH_3COCH_3)_nH^+$,[12] $(CH_3OH)_nH^+$,[13] $(CH_3OCH_3)_nH^+$,[13] and a few heterocluster ions such as $[(ROH)_n(H_2O)_m]H^+$[14,15] and $[(CH_3OH)_n(H_2O)_m]H^+$,[16]} there are few reported cases of chemical reactions taking place within the cluster ion itself.[12,16-20] Yet it has been known that electron impact ionization of clusters leads to ions that closely resemble many of the intermediates found in bimolecular ion-molecule reactions.[21,22]

In addition to the typical unimolecular and bimolecular gas-phase chemistry already studied within clusters, our group has recently observed the generation of new cluster product ions which cannot be explained by either of these two known processes. That is, we observe product ion formation that has absolutely no counterpart with gas-phase bimolecular reactions and which only occurs within a van der Waals cluster[23]. These new processes, which we have begun to document in the past three years at the University at Buffalo, include the generation of $(C_2H_4F_2)_{n\geq4}H^+$ ions from 1,1-difluoroethane clusters[24], the generation of $(CH_3OCH_3)_nH_3O^+$ & $(CH_3OCH_3)_nCH_3OH_2^+$ ions from dimethyl ether clusters[25,26], the generation of $(NH_3)_nN_2H_5^+$ ions from ammonia clusters[27] and the photogeneration of MoO^+ and MoO_2^+ ions from van der Waals clusters of molybdenum hexacarbonyl[28]. The observation of these new chemical processes which occur only within a cluster is particularly exciting for

chemists in that we may now utilize clusters as a novel reaction medium in which to produce new molecules that could not be produced be any other means.

Thus, while the study of reactive processes in clusters may be utilized as a bridge between the gas-phase "bimolecular" and the "solvated multimolecular" world of chemical reactions in condensed phases, we feel that this bridge has in fact turned into a crossroads. That is, we have demonstrated new chemical reactions and unexpected dynamics which can occur only within the solvating environment of a cluster, either through: 1) stabilization of an unstable reagent via solvation, 2) providing new chemical pathways or 3) stabilization of an unstable intermediate via solvation. In this paper we will present illustrative examples of these three types of cluster chemistry.

B) Experimental Section

The majority of our experiments consist of generating a beam of neutral van der Waals clusters and then, by electron impact, performing mass spectroscopy on the ion cluster species generated within the molecular beam. Though the cation within the cluster is rapidly generated ($\sim 10^{-14}$ s), it takes microseconds before the generated cluster ion is mass selected by the quadrupole filter. On such a lengthy time scale the cation within the cluster may rid itself of its excess energy either by fragmentation, evaporation of neutral monomers or the solvated cation may chemically react with one (or more!) of the solvating neutrals. In any case, a new product cluster ion has been generated, which is then detected via mass spectroscopy.

One may therefore visualize the electron impact ionizer of our mass spectrometer as a 'reaction cell' in which the precursor cluster ion is generated and allowed to 'incubate' for microseconds. After this time period, the newly generated product cluster ions are subsequently analyzed via mass spectroscopy. By observing the distribution of product cluster ions in the mass spectra, we can deduce the ion-molecule chemistry which has occurred within the bulk cluster, and see how this chemistry changes as a function of cluster size.

Our molecular beam apparatus consists of a Campargue-type beam source which has been described previously[29]. The cluster beam is generated from a neat expansion through a 250 μm orifice. The mass spectrometer is an Extrel C-50 (200 W, 3/8'' diameter rods, open design ionizer) capable of unit mass resolution and uniform sensitivity up to $m/z = 1400$. During beam operation the pressure in the mass spectrometer chamber is kept below 5×10^{-7} torr.

For the metal hexacarbonyl experiments (section C-2-d) a different beam apparatus is used. Helium, seeded with an appropriate metal carbonyl compound at its room temperature vapor pressure (typically a few hundred mTorr), is admitted into the low-volume stagnation region of a Newport BV-100 pulsed molecular beam valve fitted with an end plate having a 0.5 mm diameter, 30° conical aperture. Metal hexacarbonyl van der Waals complexes are then formed in the free-jet expansion of the pulsed beam of seeded helium. Operation of the valve at 1 Hz leads to maximum chamber pressures of about 3×10^{-6} Torr. The cluster beam pulse is directed axially into the ion source of a Dycor M200M quadrupole mass spectrometer, where it is intersected by the focused output from a Lambda Physik EMG 150 excimer laser, operated on the KrF* transition at a pulse energy of ca. 100 mJ.

C) Results and Discussion

1) Stabilizing an Unstable Reagent within a Cluster

a) 1,1-Difluoroethane Clusters[24]

The dominant reactive process which occurs within the majority of cluster ions ($M_{n-1}M^+$, where M is the monomeric unit) consists of a bimolecular reaction between the monomer cation and one of the neutral solvent molecules generating a protonated cluster ion via ejection of a neutral radical (R). This

$$M_{n-2} [M + M^+] \rightarrow M_{n-1}H^+ + R \qquad (1)$$
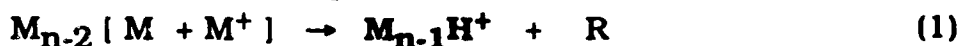
class of reactions has been well studied in a variety of bimolecular gas phase experiments and is observed to occur for a wide range of molecules. In most cases this reaction is highly exoergic and quite facile. Therefore, a molecular cluster mass spectrum is dominated typically by the appearance of cluster ions with the general empirical formula $M_{n-1}H^+$.

However, for many organic molecules, upon electron impact ionization, the parent ion is not observed mass spectroscopically. That is, the ground state cation (M^+) is thermodynamically unstable with respect to fragmentation. In such cases the mass spectrum is then composed solely of fragment ions, and identification of this molecule must be made by the characteristic fragmentation pattern.

The mass spectrum of 1,1-difluoroethane (DFE) represents just such a case. Since the parent ion is unstable, we would expect that the protonation reaction (reaction 1) not to occur within the DFE cluster ion, since the parent ion does not survive long enough to react with one of the solvating monomers. Hence, the cluster mass spectrum of DFE should have a complete absence of peaks with the formula $M_{n-1}H^+$ and be composed solely of solvated fragment ions. Figure 1 shows a 100 eV mass spectrum of DFE clusters as a function of cluster size and process channel {i.e., channel 1: $M_{n-1}CH_3CFH^+$ *(loss of F)* , channel 2: $M_{n-1}C_2H_3F^+$ *(loss of HF)* , channel 3: $M_{n-1}C_2H_3F_2^+$ *(loss of H)*, and channel 4: $M_{n-1}H^+$}. We see in Figure 1 that in addition to the expected fragmentations (channels 1-3) another sequence of peaks which have the empirical formula of $M_{n-1}H^+$ appear at n > 4 and continue to become progressively prominent with increasing cluster size. This is in direct contrast to the three fragment channels which monotonically decrease with increasing cluster size.

As Jungen and co-workers point out[30], a parent ion might be observed as a metastable ion if it is formed in the Franck-Condon region of the neutral

molecule. Thus, if the parent ion is generated within the cluster, the presence of solvating molecules may stabilize it long enough, such that it can react with one of the neutral monomers via reaction 1.

The fact that the protonated cluster ions only appear for n > 4 suggests that M_5^+ is the minimum 'critical' size necessary for stabilizing the monomer ion (i.e., in the absence of any monomer evaporation). Since monomer evaporation is expected to occur (see next section), the true 'critical' size must remain in question. However, we can make the the qualitative conclusion that the unstable reagent cation is being stabilized within the cluster long enough so it can undergo reaction 1 with a solvating monomer. We hope to further study other fluorinated hydrocarbon systems in order to better understand the systematics.

2) Providing New Chemical Pathways

a) Ammonia Clusters[27]

The ammonia cluster mass spectrum has been widely studied[10,11], and is dominated by two sequences of peaks with the empirical formula $(NH_3)_{n-1}NH_3^+$ and $(NH_3)_{n-1}NH_4^+$, corresponding to the already discussed protonation reaction (reaction 1). Careful study of the mass spectrum also reveals another series of peaks which at first glance appears to have the empirical formula $(NH_3)_{n-1}NH_2^+$. That is, they result from the process of the fragmentation of a N-H bond in the NH_3^+ cation, generating the NH_2^+ fragment intact within the cluster.

A plot of the relative intensities of the $(NH_3)_{n-1}NH_2^+$ ions as a function of cluster size (n) is shown in Figure 2, for a variety of experimental conditions. A magic number, corresponding to an enhancement in the cluster ion signal, is clearly observed for the cluster ion of size n=7 which does not change upon variations in the electron impact energy (100eV-40eV), the stagnation temperature (T_0=253-313 K), or the stagnation pressure (P_0=1-5 atm, not shown). We feel then that this intensity distribution is due solely to the large stability of the $(NH_3)_6NH_2^+$ cluster ion.

This is a very surprising result in that magic numbers[10,11] usually result from the closing of the first solvent shell around the central cation. For example, in the case of the protonated ammonia cluster ion, n = 5 is observed to be especially stable (i.e. $(NH_3)_4NH_4^+$). The unique stability of this particular cluster ion comes about from the hydrogen bonding of 4 NH_3 molecules directly to the central NH_4^+ cation[10,11]. We may now ask, if the central cation in our case is

indeed NH_2^+, why does the first solvent shell closure need 6 NH_3 molecules? Why wouldn't 2 or even 3 ammonia's suffice?

We can account for the observed size dependence of the $(NH_3)_{n-1}NH_2^+$ cluster ion yield if we assume that an associative ion-molecule reaction occurs between the nascent NH_2^+ ion and an adjacent NH_3 solvent molecule within the cluster of the form:

$$NH_2^+ + NH_3 \rightarrow N_2H_5^+ \qquad \Delta H° = -4.52 \text{ eV}[31] \qquad (2)$$

A similar (albeit endothermic) bimolecular reaction is known to occur between NH_3^+ and NH_3:

$$NH_3^+ + NH_3 \rightarrow N_2H_5^+ + H, \qquad \Delta H° = 1.12 \text{ eV}[31] \qquad (3)$$

at a rate which is about 0.1% of gas-kinetic.[32] We expect the barrier for reaction (2) to be smaller than that for reaction (3) for the following reasons. First, within the context of the Hammond postulate,[33] the barrier to reaction (2) is expected to occur earlier along the reaction coordinate, the potential surface is expected to be more attractive, and the transition state is expected to more closely resemble the reactants. Second, the activation energy for reaction (2) is expected to be lower than that of reaction (3), since the transition state for (3) must contain at least one highly extended N-H bond (correlating with eventual loss of the product H atom). By analogy with other associative bimolecular reactions, we would expect the activation energy for reaction (2) to be small, if not negligible, and determined to a great extent by the dipole-dipole interaction. We might therefore expect, based on differences in activation energies and Arrhenius A factors, that the associative reaction (2) will proceed at a rate significantly greater than 0.1% of the gas-kinetic rate.

While the "naked" (unclustered) product of the highly exothermic associative reaction (2) would have sufficient internal energy to undergo subsequent N-H bond cleavage, it would certainly be stabilized through solvation by additional NH_3 molecules. In fact, if we hydrogen-bond five NH_3 solvent molecules to the five H atoms of the $N_2H_5^+$ product ion, we end up with an ion having a completed solvation shell with the anticipated empirical formula, $(NH_3)_6NH_2^+$. The proposed $(NH_3)_5N_2H_5^+$ structure is illustrated in Figure 3. This cluster ion has a total of seven nitrogen atoms and accounts for our observation of a magic number at n=7. It is expected that the large exothermicity of reaction (2) should enhance this magic number effect, since the excess heat will serve to "boil off" the loosely bound solvent molecules which are not in the first solvent shell. This is an interesting example wherein the observation of magic numbers was necessary to elucidate the true chemical identity of the central cation.

As shown in Figure 4, if we reduce the nozzle diameter (250μm vs. 50μm) or change the expansion mixture (neat NH_3 vs. 3% NH_3 in He) the magic number

at n=7 disappears! [34] An explanation for this effect lies in that conditions of smaller aperture size and a seeded expansion both make for inefficient clustering. The distribution of neutral cluster sizes will be concentrated more toward small n. This would certainly suggest that the $(NH_3)_5N_2H_5^+$ cluster ion was originally generated from an extremely large neutral cluster. Following electron impact to form the NH_2^+ cation, this cluster must undergo many successive fragmentation/evaporation processes, until finally achieving a structure consisting of a closed solvent shell of 5 ammonia molecules hydrogen bonded to a central cation, the protonated hydrazine.

Inspired by this result, Buck, Krohne and Linnartz[35] have performed new experiments which involve first mass selecting their neutral ammonia cluster beam through a crossed molecular beam expansion. Their work indicates that neutral clusters of n > 25 are necessary in order to observe the magic number for the $(NH_3)_4NH_4^+$ cation. This new result demonstrates the significant amount of monomer evaporation which can occur within the cluster following the initial ionization/reaction event,
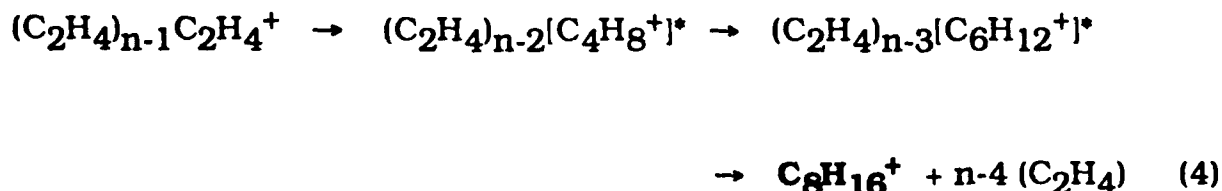
b) Ethylene Clusters[36]

The ethylene cluster mass spectrum is quite simple in that it is composed of a single sequence of cluster ions with the formula $(C_2H_4)_n^+$, which one would naturally attribute to the unreacted parent cluster ion. Figure 5 shows the intensity distributions of this sequence of cluster ions, $(C_2H_4)_n^+$ as a function of nozzle temperature. We observe that at decreased nozzle temperature (or increased stagnation pressure, 1.5-3.5 atm)[36] a very pronounced magic number appears for the empirical formula $(C_2H_4)_4^+$.

This observation of n=4 being a magic number only under certain expansion conditions is difficult to explain solely in terms of stabilities of either the neutral or ionic parent ethene clusters. In the previous discussion of ammonia clusters, a closed solvent shell hydrogen bonded to a central cation was the driving force for the appearence of a magic number. In a system, such as ethylene, where hydrogen bonding does not play a significant role, the observation of pronounced magic numbers is not expected since the distribution of neutral clusters is produced by processes which are essentially statistical in nature (i.e., why should the $(C_2H_4)_4^+$ cluster ion be so stable?). There would seem to be no *a priori* reason to predict that any particular ethylene cluster size should be extraordinarily stable. If magic numbers were observed in such a system, it seems logical that the thermodynamic stabilities of the daughter ion cluster or neutral cluster parent would not be the controlling factors.

High pressure mass spectroscopy[37] has shown that the $C_2H_4^+$ cation undergoes an exothermic condensation reaction with a neutral C_2H_4 molecule to form a branched $C_4H_8^+$ cation. This new $C_4H_8^+$ cation can then undergo successive reactions with additional C_2H_4 molecules to form a larger and larger branched cation with the general formula $C_{2m}H_{4m}^+$. The rate of each successive condensation reaction decreases rapidly as the extent of the branching of the product cation increases and has been attributed to steric effects.[37]

We now speculate that the ethylene cluster ions we observe represent the products of a similar series of intracluster condensation reactions. The observation of the magic number at n = 4 (under expansion conditions which create extensive clustering) is therefore due to the formation of the $C_8H_{16}^+$ molecular ion generated via a series of succesive ion-molecule reactions within the cluster. Since these condensation reactions are exothermic[38] we would then also expect extensive evaporation of unreacted monomers (as seen before with the ammonia system).

In summary, neutral $(C_2H_4)_n$ clusters with n > 4, following ionization via electron impact, react to give primarily $C_8H_{16}^+$ as shown in reaction (4).

$$(C_2H_4)_{n-1}C_2H_4^+ \;\rightarrow\; (C_2H_4)_{n-2}[C_4H_8^+]^* \;\rightarrow\; (C_2H_4)_{n-3}[C_6H_{12}^+]^*$$

$$\rightarrow\; C_8H_{16}^+ + n\text{-}4\,(C_2H_4) \qquad (4)$$

The intensity of these ions would then be expected to increase as the distribution of the neutral ethylene clusters grows larger (i.e., as either $T_0 \downarrow$ or $P_0 \uparrow$: n $\uparrow$). The prominent peak at n = 4 represents a balance between two competing effects: the larger the cluster the greater the probability of reaction 4, however, as the cluster size increases the rate constants of each individual step decrease. This is a new interpretation in that this particular magic number is attributed not to a central cation solvated by neutral monomers but rather due to the generation of a new molecular ion.

c) Ar-Methanol Clusters[39]

For neat methanol expansions or He-seeded methanol expansion, the cluster mass spectrum looks exactly the same, a single sequence of peaks with the formula $(CH_3OH)_nH^+$ resulting from the intracluster protonation reaction which was discussed previously (reaction 1). However, with an Ar-seeded methanol expansion we see, in addition to that sequence of peaks, a multitude of others,

which become more prominent at low electron energy (< 20 eV) and are shown in Figure 6. Most of these new peaks are attributed to cluster ions of the formula $Ar_n(CH_3OH)_m^+$, cluster ions in which the protonation reaction **does not** occur.

It is interesting to note that the sequence of peaks with the general formula $Ar_n(CH_3OH)^+$ is the only heroclutser sequence which exhibits a series of fragment peaks (ie. $Ar_nCH_2OH^+$, $Ar_nCH_2O^+$, Ar_nCHOH^+ etc.). Intriguingly enough the appearence potentials (AP) for all of these cluster ions fall in the same region (11.3eV-11.8eV) which we take as an indication that these fragments arise from similar precursors.

For this particular herocluster a large difference exists between the ionization potentials of the two components (i.e., $IP(CH_3OH) = 10.85$ eV vs. $IP(Ar) = 15.76$ eV). In such a case, at electron energies below the IP(Ar) one would expect direct vertical ionization of the methanol component. In other herocluster systems, workers[40,41] have proposed that the ionization of the molecular component of an argon-herocluster is mediated by the argon. That is, for the case of low electron energies, the Ar is first electronically excited (via electron impact) and this excitation energy is subsequently transferred to the molecular component via 'intracluster Penning ionization'. After the ionization, any excess energy can then go to promote fragmentation of the methanol ion.

We feel that our measured AP's can be taken as strong evidence for the direct participation of an excited state of Ar ($^3P_{2,0}$:11.55 eV) resulting in the eventual ionization of the argon/methanol clusters. This represents the first time intracluster Penning ionization has been identified using electron impact measurements. Regardless of the details of the ionization mechanism, it is apparent that the chemistry of the molecular components in Ar/CH_3OH heroclusters is substantially altered relative to that of neat CH_3OH or He/CH_3OH expansions due to the direct mediation of the Ar atom.

d) Metal Hexacarbonyl Clusters [28]

Van der Waals clusters of $M(CO)_6$ (M=Mo, W) generated in the free-jet expansion of a pulsed beam of seeded helium are subjected to multiphoton ionization (MPI) and the product ions analyzed by quadrupole mass spectrometry. These species are of fundamental significance in our understanding of metal-metal and metal-ligand bonding interactions, and can serve as models for the study of catalysis and surface phenomena. Studies of the effects of cluster size and structure on reactivity of transition metal carbonyl clusters can provide us also with the necessary database to test and refine our theories concerning the chemistry and physics of bulk metals.

The multiphoton dissociation and ionization dynamics of mononuclear and covalently bound multinuclear transition metal carbonyls is well understood: initial multiphoton dissociation (MPD) of the metal carbonyl results in complete ligand stripping, leaving behind a naked metal atom which is subsequently photoionized. Consequently, the 248 nm. MPI mass spectrum for the $M(CO)_6$ monomer is dominated almost exclusively by the M^+ cation signal.

On the other hand, the multiphoton photophysics of van der Waals complexes of transition metal carbonyls is not so thoroughly characterized. Indeed, for MPI of $\{M(CO)_6\}_n$ clusters, we observe not only the production of M^+ but the oxide ions; MO^+ and MO_2^+. Observing the production of these ions as a function of laser intensity reveals that the yield of M^+ depends on the square root of laser intensity, while the yields for both of the oxide ions are found to be nearly independent of laser intensity (6-210 mJ). This strongly suggests that the mechanism leading to production of M^+ remains sensitive to laser intensity over the range of intensities investigated, while the mechanism leading to production of the metal oxide ions is nearly saturated within this range of intensities. Therefore, we conclude that we are probably observing two distinct processes. The first is a multiphoton dissociation within the cluster leading to a bare metal atom which is subsequently ionized via MPI, generating the M^+ ion signal. The second process is a photochemically induced intracluster reaction leading to oxomolybdenum ions.

We propose that a novel binuclear adduct arises thru an intracluster reaction and that the oxide ions arise thru subsequent photoionization and fragmentation of that adduct. That is, within the cluster, the photogenerated metal atom can associate with the ligands of an adjacent metal carbonyl "solvent" molecule. We therefore propose, on the basis of orbital symmetry considerations, that the nascent metal "photoatom" interacts with a neighboring metal carbonyl "solvent molecule" via two such bridging carbonyls to form a stable six member structure. Then through back-donation of metal d_{xy} electron density to the empty π^* MO's of the carbonyl ligands, the 2 C-O bonds weaken and break, eventually resulting in the observed oxide ion formation.

However, we find no evidence of such behavior in the $Cr(CO)_6$ system. Based on these results for the group VI B hexacarbonyls, we suggest that the reactivity within clusters of first-row transition metal atoms is fundamentally different from that of second- or third-row metals and is determined by the occupancy and relative size of the metal d orbitals. Based on our model we would predict that the intracluster reaction between a photogenerated metal atom and an adjacent $M(CO)_6$ cluster molecule depends explicitly on the efficient overlap of the relevant molecular orbitals. For Cr, the small d orbital on

the metal makes for poor overlap wit'. :he carbonyl ligands, hence the lack of reactivity. This model, which invokes different modes of CO coordination, may have important implications for the study of catalysts.

3) Stabilizing an Unstable Intermediate within a Cluster

a) Dimethyl Ether Clusters[25,26]

The bottom panel of Figure 7 shows a typical 70 eV electron impact mass spectrum for $(CH_3OCH_3)_n$ clusters extending from the dimer to the trimer. In addition to the expected protonated cluster peaks there are other peaks corresponding to the hydronium ion (which has been reported previously[25]) and protonated methanol ions, solvated by 2 dimethyl ether (DME) molecules. This sequence of cluster peaks is observed throughout the entire cluster mass spectrum.

It is interesting to note that while the CH_3^+ *(loss of CH_3O)* & $CH_3OCH_2^+$ *(loss of H)* fragment cations are extremely intense in the monomer mass spectrum of DME (~ 54% of all ion intensity), the same cluster cations are substantially reduced in intensity (i.e., $(DME)_nCH_3^+$ & $(DME)_nCH_3OCH_2^+$). We speculate that this is due to the fragments being consumed by a chemical reaction within the cluster. A likely candidate is the ion-molecule reaction of the fragment cations with a neutral DME, within the cluster, to form a trimethyloxonium cation intermediate. This type of ion-molecule reaction has been previously observed by Harrison and Young through the use of a tandem mass spectrometer[42]. The newly formed trimethyloxonium cation may then undergo a rearrangement to form the observed products. This reaction mechanism is illustrated in Figure 7.

The mechanism is similar to that observed for the decomposition of DME over zeolite catalysts. van Hooff, *et al.*[43] observed that conversion of DME over a zeolite catalyst produced ethylene and propene as primary olefins. To account for their results they invoked a trimethyloxonium intermediate as the common intermediate for the observed products. We therefore speculate that the DME cluster reactions leading to the same products should involve the same mechanism found to occur on zeolite catalysts. That is, within the stabilizing environs of a cluster, the trimethyloxonium cation may internally rearrange where it then forms protonated methanol (via elimination of ethylene) or protonated water (via elimination of propene).

This analogous process has previously been reported for the collisional activation of the monomer $(CH_3)_3O^+$ ion[44]. However recent additional work

appears to be at variance with that original result[45]. This variance we feel is due to the thermodynamic instability of the bare $(CH_3)_3O^+$. For the isolated $(CH_3)_3O^+$, unimolecular dissociation can now effectively compete with the rearrangement reaction, and only simple methyl loss is observed. However, within the solvating environs of a cluster (or a zeolite surface), this unstable intermediate may be stabilized on a long enough time scale to now allow it to undergo this rearrangement reaction, to then form the observed products.

b) Photodissociation of Cr(CO)$_6$ within a Methanol Cluster[46]

It is well known that 248 nm. multiphoton ionization (MPI) of gas phase Cr(CO)$_6$ monomer results primarily in the formation of the Cr^+ cation. This phenomon occurs due to the metal hexacarbonyl first absorbing 2 or 3 photons and then undergoing MPD causing the metal center to lose all 6 CO ligands, with the excited bare metal atom being subsequently photoionized. Tyndall and Jackson[47] have proposed the following scheme for sequential photo-dissociation at 248 nm under collisionless conditions:

$$Cr(CO)_6 + h\upsilon \dashrightarrow Cr(CO)_4^* + 2\ CO \qquad (5a)$$
$$Cr(CO)_4^* + h\upsilon \dashrightarrow Cr(CO)_2 + 2\ CO \qquad (5b)$$

They also described a direct, non-sequential process in which Cr(CO)$_6$ is excited into a dissociative continuum via two- or three-photon absorption, giving rise to several excited states of atomic chromium:

$$Cr(CO)_6 + (\geq 2\ h\upsilon) \dashrightarrow Cr^* + 6\ CO \qquad (6)$$

which is apparently important at higher fluences.

This is not the case in solution[48], where the Cr(CO)$_6$ undergoes single ligand loss to generate Cr(CO)$_5$. Results from transient visible absorption experiments are consistent with the following scheme for the photodissociation of Cr(CO)$_6$ in solution:

$$Cr(CO)_6 + h\upsilon \dashrightarrow Cr(CO)_6^* \qquad (7)$$
$$Cr(CO)_6^* \dashrightarrow Cr(CO)_5^* + CO \qquad (8)$$
$$Cr(CO)_5^* + S \dashrightarrow S\bullet Cr(CO)_5^* \qquad (9)$$
$$S\bullet Cr(CO)_5^* \dashrightarrow S\bullet Cr(CO)_5 \qquad (10)$$

where S denotes a solvent molecule and the asterisk denotes an internally excited species.

To probe the intermediate regime between the two extremes of gas-phase and solution behavior, we decided to study the 248 nm. MPI mass spectrum of Cr(CO)$_6$ solvated within a cluster. In particular, we wished to observe the photodynamics of the S_nCr(CO)$_6$ species, where the S stands for a methanol molecule. To do this we first bubbled the He carrier gas through a reservoir

containing methanol, before passing this gas over the solid $Cr(CO)_6$. We then expanded the resulting mixture through the same pulsed valve used before, but now employing a newly constructed time-of-flight mass spectrometer (TOFMS) which has expanded considerably our mass range.

The MPI spectrum is shown in Figure 8a and is clearly much more complex than one might first expect. The plethora of ion peaks can be ascribed to a general empirical formula $S_n\{Cr(CO)_x\}^+$ where again S is the CH_3OH molecule and x = 0,1,2,5,6. Clearly there are many more species here than just the solvated Cr^+ cation.

The major sequence of cluster ions $[S_nCr(CO)_x^+ (x = 0,1,2)]$, we feel are formed first via a two-photon dissociation of the $S_nCr(CO)_6$ to give as a primary excited **neutral** photoproduct $S_nCr(CO)_4^*$. Following this photodissociation, there is an additional two-photon nonresonant ionization of the $S_nCr(CO)_2^*$, to then give $S_nCr(CO)_2^+$, as well as S_nCr^+, and $S_nCr(CO)^+$.

The second sequence of cluster ions with the empirical formula, $S_nCr(CO)_x^+$ (x = 5,6) are fromed first via a two-photon ionization of $S_nCr(CO)_6$ giving rise to the excited **ion**, $S_n[Cr(CO)_6^*]^+$. This energized cluster ion may then relax, in a liquid-like fashion, by V-V energy transfer to the methanol 'bath' molecules, to give the $S_n[Cr(CO)_6]^+$ cluster ion. In addition, there is also a second competing relaxation process which is dissociation of a single CO ligand, to form $S_nCr(CO)_5^+$.

To test this hypothesis further we again looked at the 248 nm. MPI TOFMS of $Cr(CO)_6$ but now complexed with deuterated methanol. As shown in Figure 8b we observe a series of peaks which can again be given the general formula $S_n\{Cr(CO)_x\}^+$, but now for x = 0,1,2,6 (i.e, the sequence corresponding to $S_n\{Cr(CO)_5\}^+$ is absent). This change in the MPI mass spectra of $Cr(CO)_6/CH_3OH$ clusters and $Cr(CO)_6/CD_3OD$ clusters we attribute to the differing efficiencies of CH_3OH and CD_3OD for relaxation of the excited $[Cr(CO)_6^*]^+$ photoions through intracluster V-V energy transfer. It would appear that with CD_3OD the isotopic shift in vibration frequencies now allows for efficient V-V energy transfer, thereby allowing easy stabilization of the excited nacent photoion and only $\{CD_3OD\}_nCr(CO)_6^+$ is observed.

15

D) Future Directions

The examples just discussed represent a sampling of the new cluster chemistry which we have recently observed and which can also occur within multiply charged cluster ions as well[49]. We feel this is only the beginning in terms of the new chemistry which can be discovered within clusters. New experimental directions we hope to employ in the near future include the use of mass selected cluster beams to directly observe cluster reaction dynamics, and to spectroscopically probe, via laser induced flourescence, the internal states of the radical product generated via these cluster reactions.

References

(1) Whitehead, J. C.; Grice, R. *Faraday Discuss. Chem. Soc.* **1973**, *55*, 320.

(2) King, D. L.; Dixon, D. A.; Herschbach, D. R. *J. Am. Chem. Soc.* **1974**, *96*, 3328.

(3) Gonzalez Urena, A.; Bernstein, R. B.; Phillips, G. R. *J. Chem. Phys.* **1975**, *62*, 1818.

(4) Behrens, R. B., Jr.; Freedman, A.; Herm, R. R.; Parr, T. P. *J. Chem. Phys.* **1975**, *63*, 4622.

(5) Wren, D. J.; Menzinger, M. *Chem. Phys.* **1982**, *66*, 85.

(6) Nieman, J.; Na'aman, R. *Chem. Phys.*, **1984**, *90*, 407.

(7) Morse, M. D.; Smalley, R. E. *Ber. Bunsenges. Phys. Chem.* **1984**, *88*, 208.

(8) Whetten, R. L.; Cox, D. M.; Trevor, D. J.; Kaldor, A. *Surf. Sci.* **1985**, *156*, 8.

(9) Hermann, V.; Kay, B. D.; Castleman, A. W., Jr.; *Chem. Phys.* **1982**, *72*, 185.

(10) Stephan, K.; Futrell, J. H.; Peterson, K. I.; Castleman, A. W., Jr.; Wagner, H. E.; Djuric, N.; Märk, T. D. *Int. J. Mass Spectrom. Ion Phys.* **1982**, *44*, 167.

(11) Echt, O.; Morgan, S.; Dao, P. D.; Stanley, R. J.; Castleman, A. W., Jr. *Ber. Bunsenges. Phys. Chem.* **1984**, *88*, 217.

(12) Stace, A. J.; Shukla, A. K. *J. Phys. Chem.* **1982**, *86*, 865.

(13) Grimsrud, E. P.; Kebarle, P. *J. Am. Chem. Soc.* **1973**, *95*, 7939. Morgan, S.; Castleman, A. W, Jr. *J. Phys. Chem.* **1989**, *93*, 4544. Ibed., *J. Am. Chem. Soc.*, **1987**, *109*, 2868.

(14) Stace, A. J.; Shukla, A. K. *J. Am. Chem. Soc.* **1982**, *82*, 5314.

(15) Stace, A. J.; Moore, C. *J. Am. Chem. Soc.* **1983**, *83*, 1814.

(16) Walters, E. A.; Grover, J. R.; White, M. G; Hui, E. T. *J. Phys. Chem.* **1987**, *91*, 2758.

(17) Klots, C. E.; Compton, R. N. *J. Chem. Phys.* **1978**, *69*, 1644, Klots, C. E. *Radiat. Phys. Chem.* **1982**, *20*, 51. Ibed. *Kinetics of Ion-Molecule Reactions*; Ausloos, P., Ed.; Plenum: New York, 1979; p 69.

(18) Ono, Y.; Ng, C. Y. *J. Am. Chem. Soc.* **1982**, *104*, 4752.

(19) Nishi, N.; Yamamoto, K.; Shinohara, H.; Nagashima, U.; Okuyama, T. *Chem. Phys. Lett.* **1985**, *122*, 599.

(20) Stace, A. J. *J. Am. Chem. Soc.* **1985**, *107*, 755.

(21) Milne, T. A.; Beachey, J. E.; Greene, F. T. *J. Chem. Phys.* **1972**, *56*, 3007.

(22) Ceyer, S. T.; Tiedemann, P. W.; Ng. C. Y.; Mahan, B. H.; Lee, Y. T. *J. Chem. Phys.* **1979**, *70*, 2138.

(23) Garvey, J. F.; Bernstein, R. B. *Chem. Phys. Lett.* **1986**, *126*, 394, Garvey, J. F.; Bernstein, R. B. *J. Phys. Chem.* **1986**, *90*, 3577.

(24) Coolbaugh, M. T.; Peifer, W. R.; Garvey, J. F. *J. Phys. Chem.* **1990**, *94*, 1619.

(25) Garvey, J. F.; Bernstein, R. B. *J. Am. Chem. Soc.* **1987**, *109*, 1921.

(26) Coolbaugh, M. T.; Peifer, W. R.; Garvey, J. F. *J. Am. Chem. Soc.* **1990**, *112*, 3692.

(27) Peifer, W. R.; Coolbaugh, M. T.; Garvey, J. F. *J. Chem. Phys.* **1989**, *91*, 6684.

(28) Peifer, W. R.; Garvey, J. F. *J. Phys. Chem.* **1989**, *93*, 5906. Ibed. *Int. J. of Mass Spectrom. Ion Proc.* **1990**, in press.

(29) Campargue, R.; Lebehot, A. *9th Int. Symp. Rarefied Gas Dynamics*, Göttingen **1974**, *11*, 1. Campargue, R. *J. Phys. Chem.* **1984**, *88*, 4466.

(30) Heinis, T.; Bär, R.; Börlin, K.; Jungen, M. *Chem. Phys.* **1985**, *94*, 235.

(31) Rosenstock, H. M.; Draxl K.; Steiner, B. W.;Herron, J. T. *J. Phys. Chem. Ref. Data 6*, **1977**, Suppl. Monograph 1. Meot-Ner, M.; Nelsen, S. F.; Willi, M. R.; Frigo, T. B. *J. Am. Chem. Soc.* **1984**, *106*, 7384.

(32) Derwish, G. A. W.; Galli, A.; Giardini-Guidoni, A.; Volpi, G. G. *J. Chem. Phys.* **1963**, *39*, 1599. Melto, C. E. *J. Chem. Phys.* **1966**, *45*, 4414.

(33) Hammond, G. S. *J. Amer. Chem. Soc.*, **1955**, *77*, 334.

(34) Coolbaugh, M. T.; Peifer, W. R.; Garvey, J. F. *J. Chem. Phys.* in press.

(35) Buck, U.; Krohne, R.; Linnartz, L. *J. Chem. Phys.* in press.

(36) Coolbaugh, M. T.; Peifer, W. R.; Garvey, J. F. *Chem. Phys. Lett.* **1990**, *168*, 337,

(37) Kebarle, P; Haynes, R. M., *J. Chem. Phys.* **1967**, 47, 1676.

(38) for the reaction $C_2H_4+ + C_2H_4 \rightarrow C_4H_8^+$, $\Delta H^0 = -1.43$ to -2.60 eV depending on the structure of the product

(39) Vaidyanathan, G., Coolbaugh, M. T.; Peifer, W. R.; Garvey, J. F. *J. Phys. Chem.* submitted **1990**.

(40) Stace, A. J *J. Phys. Chem.*, **1987**, *91*, 1509.

(41) Isenor, N. R.; Qi, J. *Chem. Phys. Lett.* **1989**, *155*, 283.

(42) Harrison, A. G.; Young, A. B. *Intern. J. of Mass Spectrom. Ion Proc.* **1989**, *94*, 321.

(43) van Hooff, J. H. C.; van der Berg, J. P.; Wolthuizen, J. P.; Volmer, A. *Proc. Int. Zeolite Conf.*, 6th, **1983**, 489.

(44) Sigsby, M. L.; Day, R. J.; Cooks, R. G. Org. Mass Spectrum, **1979**, *14*, 274

(45) Farcasiu, D.; Pancirov, R.G. *Int. J. of Mass Spectrom. Ion Proc.* **1986**, 74, 207

(46) Peifer, W. R.; Garvey, J. F. *J. Chem. Phys.*, submitted **1990**.

(47) Tyndall, G. W.; Jackson, R. L. *J. Chem. Phys.* **1989**, *91*, 2881.

(48) Simon, J. D.; Xie, X. *J. Phys. Chem.* **1986**, *90*, 675.

(49) Coolbaugh, M. T.; Peifer, W. R.; Garvey, *Chem. Phys. Lett.* **1989**, *156*, 19. Ibed. *Chem. Phys. Lett.* **1990** *164*, 441, Peifer, W. R.; Coolbaugh, M. T.; Garvey, J. F. *J. Phys. Chem.* **1989**, *93*, 4700.

Figure Captions

Figure 1: Bar graph representing percent yield of daughter cluster ion as a function of cluster ion size (n) and process channel at 100 eV electron impact energy. Note how all three of the fragmentation channels decrease as a function of n (channel 1: 87%→43%, channel 2: 8%→3%, channel 3: 5%→2%) while the cluster reaction channel (channel 4) increases with n (0%→52%).

Figure 2: Intensity of $(NH_3)_{n-1}NH_2^+$ vs. cluster size, as a function of electron impact energy ($T_0 = 273K$, $P_0 = 1$ atm) and as a function of stagnation temperature (70 eV, $P_0 = 1$ atm). Note the prominent magic number at n = 7 (reprinted with permission from ref. 27).

Figure 3: Proposed structure for $(NH_3)_6NH_2^+$ cluster ion. This species is the most prevalent of all cluster ions in the series, $(NH_3)_{n-1}NH_2^+$, and is believed to be a protonated hydrazine molecule surrounded by one complete solvation shell of neutral ammonia's hydrogen bonded to the central cation (reprinted with permission from ref. 27).

Figure 4: Ion intensity of $(NH_3)_{n-1}NH_2^+$ vs. cluster size as a function of expansion conditions using 70 eV electron impact: a) nozzle size (using neat ammonia), b) expansion seeding (nozzle = 250μm). Note the loss of the magic number at n=7 for expansion conditions which restrict clustering.

Figure 5: $(C_2H_4)_n^+$ ion intensity as a function of nozzle temperature: $P_0 = 1.5$ atm, nozzle diameter = 250 μm, electron energy = 70 eV (reprinted with permission from ref. 36).

Figure 6: Raw mass spectrum from 50-275 amu for an Ar-CH$_3$OH cluster expansion at two different electon impact energies. Single peaks are assigned by the pair of numbers n,m ; corresponding to the empirical formula $Ar_n(CH_3OH)_m^+$. For peaks which occur in definite sequences, the number above the peak corresponds to n, (i.e., for either M_nH^+ or Ar_nM^+, where M = CH_3OH).

Figure 7: Proposed reaction mechanism for observed cluster ions generated through a common trimethyloxonium intermediate. Mass spectrum at bottom is for neat dimethyl ether cluster at 70 eV from dimer to trimer (80 to 140 amu). Major ion peaks are identified by their empirical formulas (M = $(CH_3)_2O$).

Figure 8a: 248 nm. TOFMS from 240-470 amu for $Cr(CO)_6$-CH_3OH cluster expansion. Number above assigned peaks corresponds to number of methanol molecules (n, where S = CH_3OH) complexed with the $Cr(CO)_x^+$ fragment (x =0,1,2,5,6).

Figure 8b: 248 nm. TOFMS from 240-470 amu for $Cr(CO)_6$-CD_3OD cluster expansion. Number above assigned peaks corresponds to number of methanol molecules (n, where S = CH_3OH) complexed with the $Cr(CO)_x^+$ fragment (x=0,1,2). Peaks corresponding to $S_nCr(CO)_6^+$ appear as trailing shoulders on the the more intense peaks assigned to $S_nCr(CO)_2^+$. Note how there are no peaks assigned for x = 5, which if present would appear midway between the $S_nCr(CO)^+$ and S_nCr^+ peaks.

$(NH_3)_{n-1} NH_2^+$

Electron Energy Dependence

Nozzle Temperature Dependence
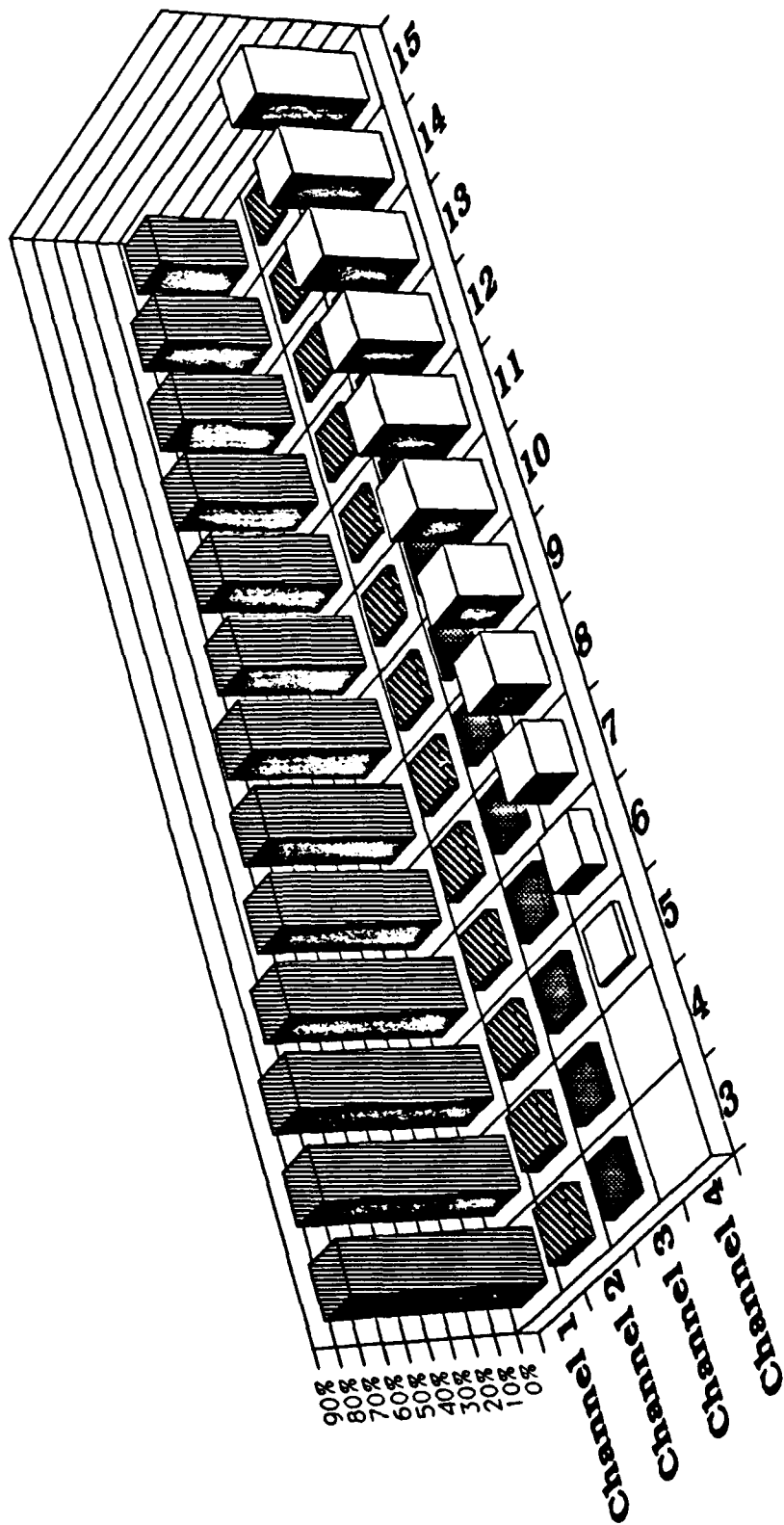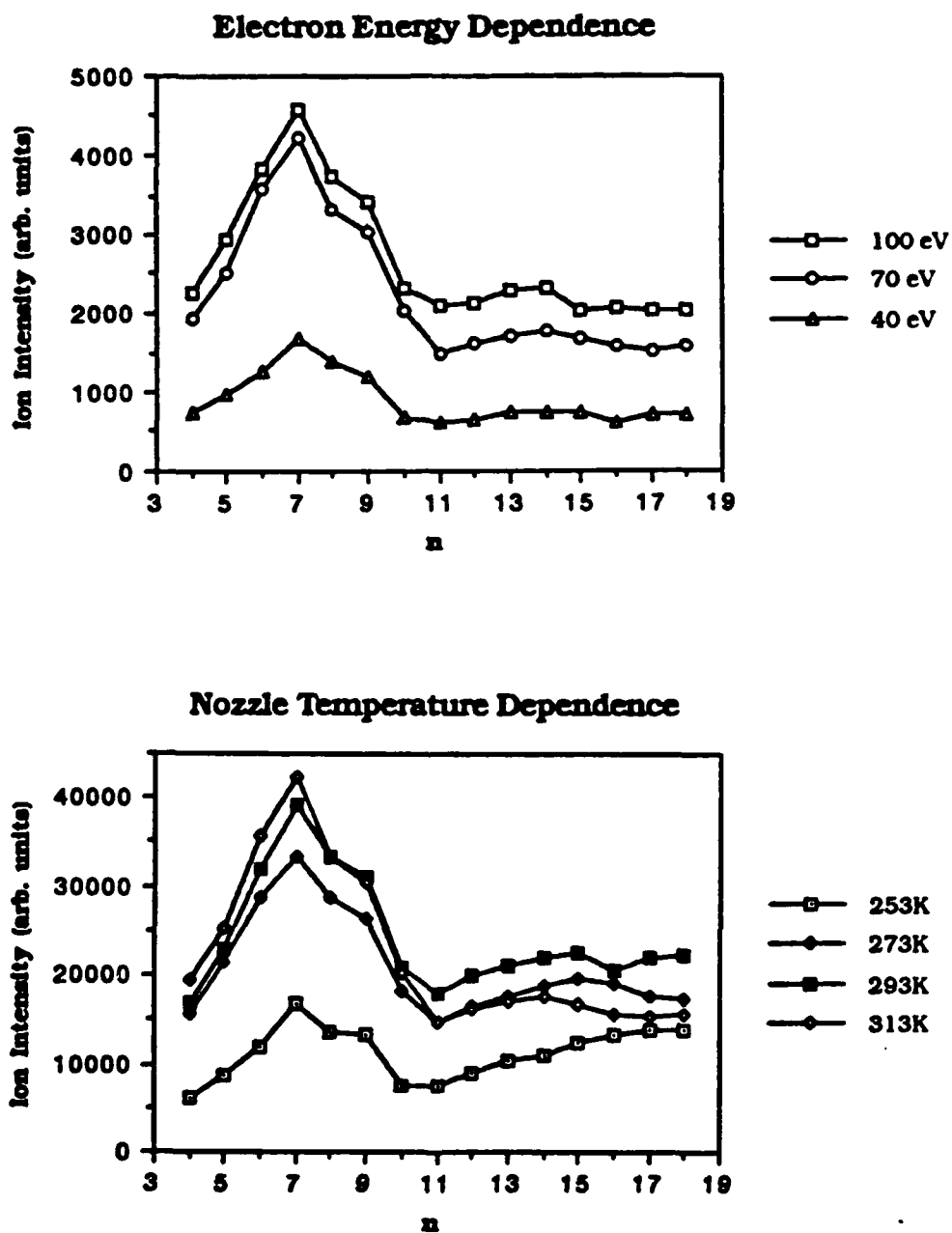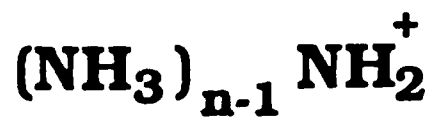
Figure 2, Garvey, et.al, "Chemistry within..."

Figure 3. Garvey, et. al. , "Chemistry within...
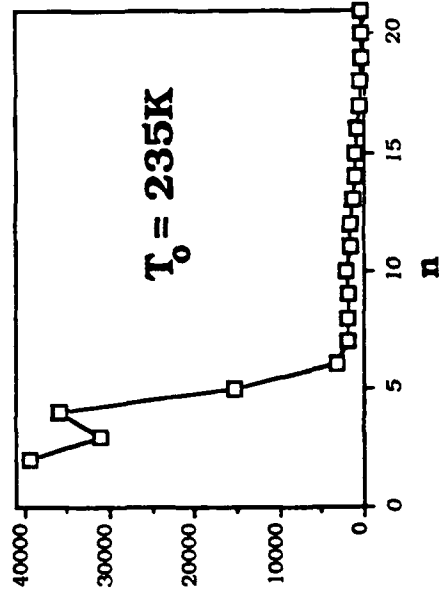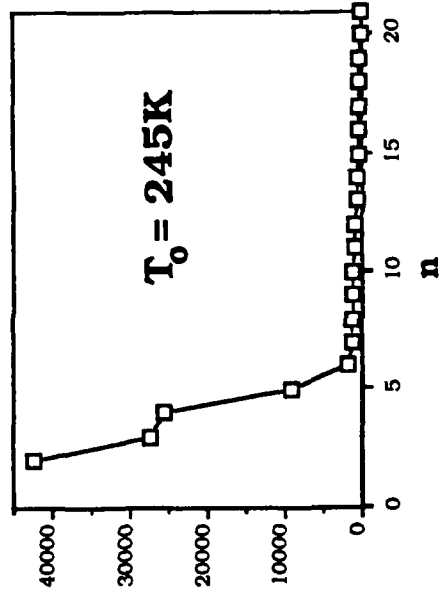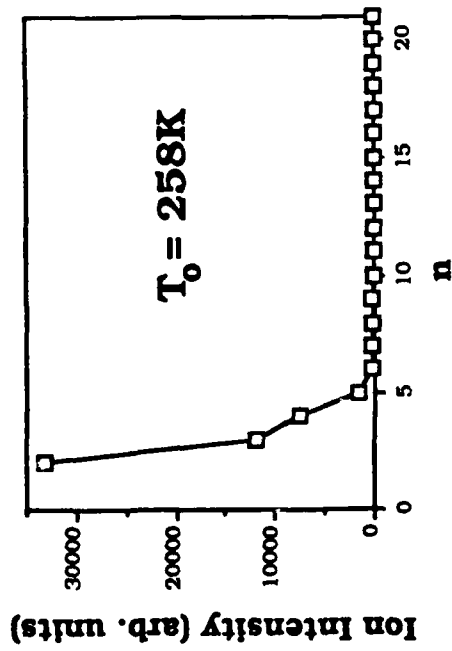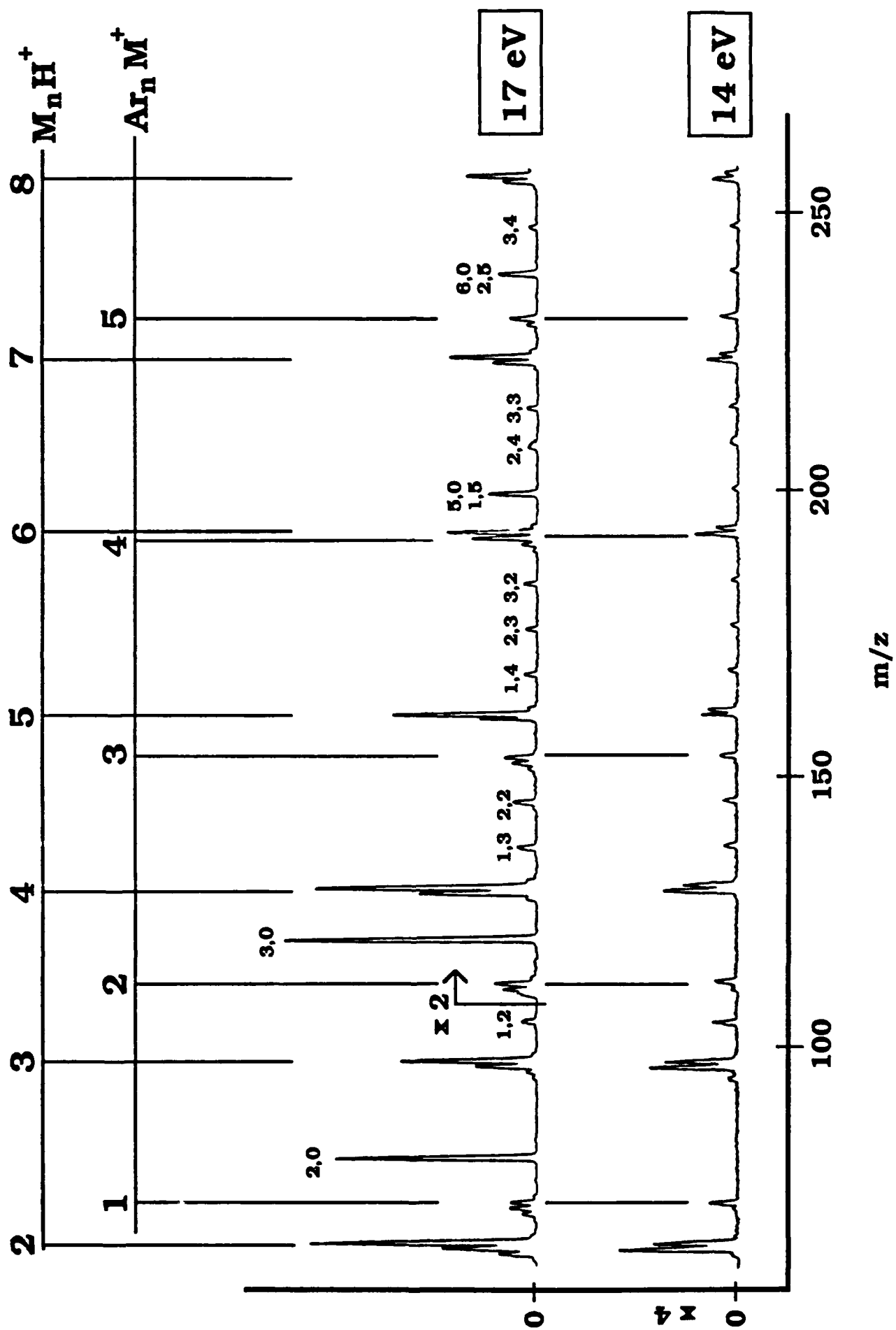
Figure 4, Garvey, et. al., "Chemistry within ,,..."

$$CH_3^+ + CH_3OCH_3 \qquad\qquad CH_3OCH_2^+ + CH_3OCH_3$$

$-CH_2O$

$$\left[\begin{array}{c} CH_3 \\ | \\ CH_3 - O\ + \\ | \\ CH_3 \end{array} \right]$$

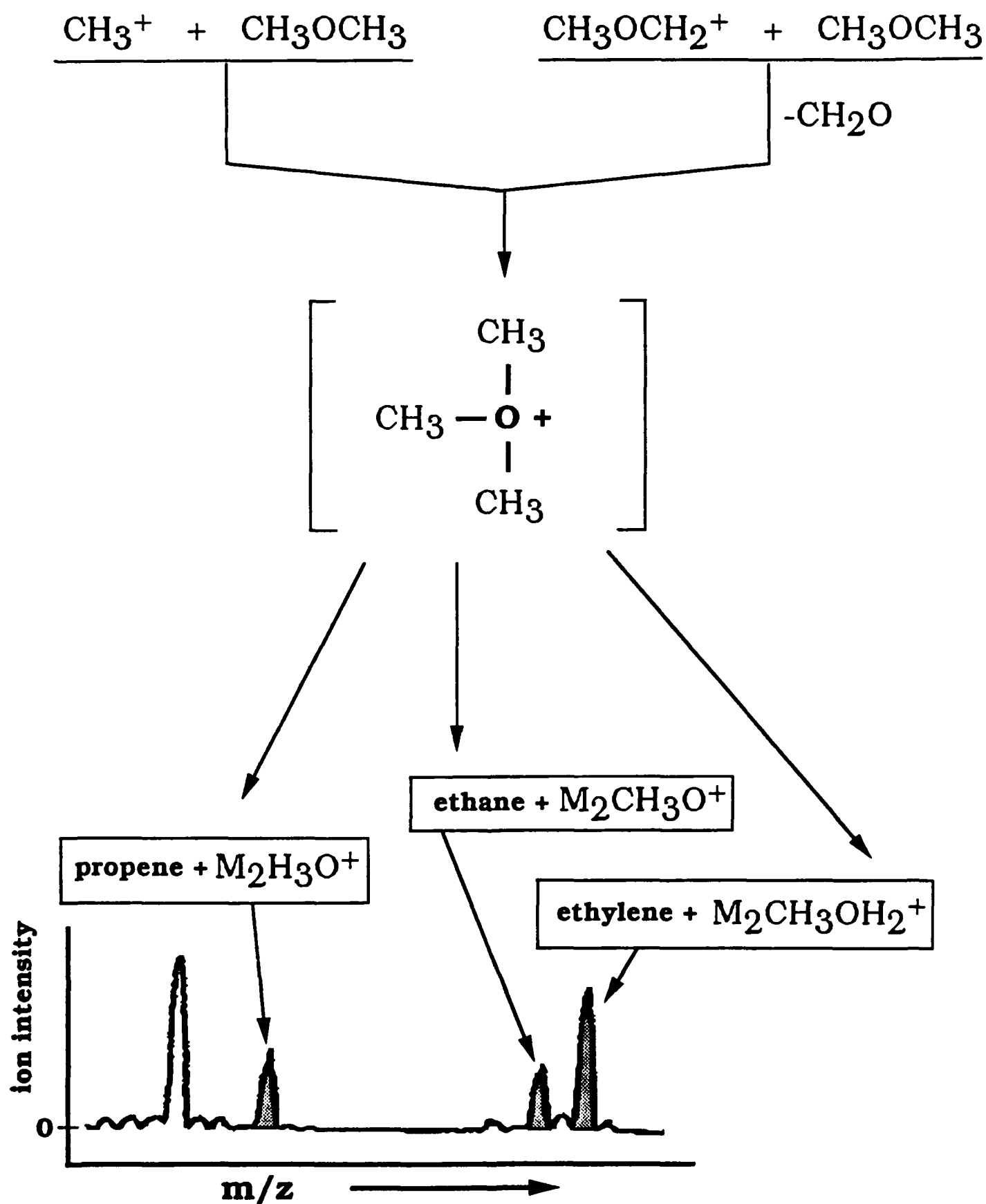propene + $M_2H_3O^+$

ethane + $M_2CH_3O^+$

ethylene + $M_2CH_3OH_2^+$

ion intensity

0

m/z

Figure 7, Garvey et. al., "Chemistry within ...

S_nCr^+

$S_nCr(CO)^+$

$S_nCr(CO)_2^+$

Ion Intensity (arb. units)

m/z